Application and validation of a viscosity approach to the existence of nanogratings in oxide glasses

Qiong Xie[1], Maxime Cavillon[1,*], Bertrand Poumellec[1], Diego Pugliese[2], Davide Janner[2], and Matthieu Lancry[1]

[1]Institut de Chimie Moléculaire et des Matériaux d'Orsay (ICMMO), Université Paris-Saclay, CNRS, 91405 Orsay, France
[2]Department of Applied Science and Technology (DISAT) and RU INSTM, Politecnico di Torino, 10129 Torino, Italy
*Corresponding author: maxime.cavillon@universite-paris-saclay.fr

Abstract

Nanogratings are self-organized and sub-wavelength birefringent structures that are formed upon the action of high intensity ultrashort light pulses in the bulk of a transparent material. They have found interest in optics/photonics, microfluidics, optical data storage or sensing applications. However, the ability to successfully imprint 3-dimensional (3D) nanogratings in silicate glasses is a strong function of the glass composition. In this work, we investigate the role of glass viscosity on the ability to induce these nanogratings. We first investigate the nanogratings formation window in an energy-repetition rate laser parameter landscape for five common oxide glasses: SiO_2 (Suprasil), GeO_2, and Schott glasses AF32, Borofloat, and BK7. Secondly, and based on previous work, we define a domain of existence of the nanogratings using viscosity-based arguments. The lower limit corresponds to a temperature at which the viscosity is ~$10^{6.6}$ Pa·s, where nanocavitation of the glass occurs, forming the nanopores that compose the nanogratings. An upper temperature limit, set for a viscosity value of ~$10^{3.0}$ Pa·s, relates to either collapse or growth of the nanopores, resulting in the erasure of the nanopores, hence the nanogratings. The experimental results agree with the predictions made by this viscosity approach and literature data. This work opens the door to future glass viscosity engineering to maximize 3D nanogratings imprinting.

I. Introduction

Nanogratings, also labeled as "Type II" transformations, were first observed in 2003 [1] after femtosecond (fs) laser irradiation inside silica glass. These nanostructures exhibit the remarkable property of being birefringent with a slow/fast axis that can be spatially controlled through light properties such as polarization. Original properties can arise from these nanostructures, such as anisotropic light scattering, linear dichroism, chiral optical properties, and high thermal stability [2], [3]. To harvest these properties and since their discovery, they have therefore driven strong interest for applications including 3D geometric phase optics and micro optical polarization sensitive elements, 5D optical data storage, microfluidics, or temperature/pressure fiber-based sensors etc. [4]–[9].

In the pioneering work of Ref. [1], the authors proposed that the existence of these sub-wavelength and pseudo-organized structures, yielding to birefringence, originated from the interference between the incident light field and the plasma induced by ultrashort laser pulses. Electronic inhomogeneities were proposed as the triggering cause of this coupling mechanism. In 2008 a transient nanoplasmonics model was introduced [10], describing the appearance of spherical nanoplasma preferentially located at the hot spots induced by localized multiphoton ionization at defects or color center locations. In this view, the nanoplasma would experience an asymmetric growth oriented preferentially in the direction perpendicular to the laser polarization, due to an asymmetric field enhancement. It would then move from a spherical to an ellipsoidal shape, and ultimately to disk-like shape, as more pulses are deposited inside the focal volume. Moreover, an exciton-polariton model was thus proposed in 2012 [11], through the coupling of light with plasmons. Later results suggested that these nanogratings originated from nanometric or sub-nanometric heterogeneities initially present in the glass, leading to coherently interfering scattering wavelets, hence the formation of a standing wave (2014: [12], and 2016: [13]). It is worth pointing out that this process is reinforced by a pulse-to-pulse effect, and both the dose and the pulse energy are key parameters in the formation of nanogratings including their pseudo-periodicity. Finally, inside the plasma dense region, the formation of porous nanolayers is observed in silica, and silica-rich glasses [14]. The nanopores constituting these nanolayers typically show a size of few tens of nm. In 2013 the presence of free molecular O_2 was detected inside

these nanopores [15]. In the same work, the birth of these nanopores was associated to a tensile stress-assisted nanocavitation and a "soft" Coulomb force necessary to overcome the oxygen binding energy and to form nanopores by recombination (to form O_2) upon an intense stress field. A cavitation mechanism was also proposed in the formation of these nanopores, building on the theory developed by Grady on spall fracture of matter [16]–[18].

A direct observation from the above introductory discussion is that the electron plasma is self-organized in hot (dense) nanoplanes, and this is *a priori* not composition limited, as it is the case for surface nanogratings (LIPSS, laser-induced periodic surface structures) [19]. While the origin(s) of nanogratings formation has not been fully elucidated yet, these features have been observed in a variety of glasses, and most specifically oxides and silica-based glasses. These include but are not limited to silica [1], [9], [20], germanosilicates [21], [22], sodium silicates [23], germania [20], [24], sodium germanates [25], alkali-free aluminoborosilicate (AF32 Schott) [26], alkali-containing borosilicate (BK7 Schott, Borofloat 33 Schott), and titanium silicate (ULE Corning) [20], [27]. However, it is worth pointing out that for some glasses such as SiO_2, GeO_2, or Borofloat 33, the laser-processing window to form nanogratings is large. On the opposite, glasses such as AF32 or likely BK7 have shown a narrower window. For BK7, only a weak birefringence response was shown, without laser-polarization dependence of the slow/fast axis orientation nor supported by electron microscope techniques demonstrating the presence of organized porous nanogratings.

In this context, this work provides insights on the relative difficulty to form nanogratings in some of these commercial glasses. The goal is to describe, based on a viscosity approach, the ability for a glass to yield permanent formation of nanogratings. First, five commercial glasses are selected, namely BK7, AF32, Borofloat 33, GeO_2, and SiO_2 (Suprasil). In addition to SiO_2 being the backbone material of many of today's photonic applications, all these glasses present interests for diverse applications. These include, among others, mid-infrared optical devices (GeO_2), silicon wafer assembly in semi-conductor industry and flat glass for display (AF32), precision optics for space telescope substrates, or photovoltaic, medical technologies (Borofloat 33), visible and near-infrared micro-optic elements, prisms (BK7). The selected glasses are then irradiated by a fs-laser and using similar conditions. This systematic work allows a direct comparison between the glass samples and their respective nanogratings processing windows. The observed differences are then tentatively linked to viscosity-driven mechanisms, framing the existence of the aforementioned nanogratings processing window. Consequently, this work is expected to establish guidelines for future glass development when nanogratings 3D structuring is required for a wide range of applications.

II. Experimental details

To investigate the effect of glass composition, hence viscosity, on the ability to form nanogratings, a series of five bulk glasses was selected based on literature results and viscosity profile (more information on this later in the paper): BK7, AF32, Borofloat 33, GeO_2, and SiO_2 (Suprasil). Each glass sample, taking the form of a plate, was irradiated in similar conditions using a femtosecond laser (Satsuma, Amplitude Système, Bordeaux, France) having a central wavelength at 1030 nm and a numerical aperture objective NA = 0.6, at a pulse duration τ_p of 800 fs. In cartesian coordinates, z is the laser beam direction, and the laser scanning irradiation was performed in the plane (x,y) perpendicular to it. This pulse duration was chosen as it corresponds to a large window of nanogratings formation in SiO_2, AF32, and Borofloat 33 [26]. In this work, the investigation of nanogratings existence was probed in a pulse energy (E_p, in µJ) – repetition rate (RR, in kHz) landscape. For all the samples excepted the BK7 glass, a constant pulse density was used (10^3 pulses/µm). Since the repetition rate is varied in this experiment, the scanning speed was varied accordingly (e.g., 10 µm/s for a RR = 10 kHz, 100 µm/s for a RR = 100 kHz, etc.). For BK7, a constant writing speed of 1 µm/s was chosen in order to enable the formation of nanogratings.

There exists a variety of possible laser-induced transformations in oxide glasses, such as formation of defects, densification, nanogratings and/or voids formation, elemental migration, partial crystallization, and appearance of a stress field [28]–[30]. Therefore, an experimental procedure must be employed to decipher if there is, or not, the presence of nanogratings inside the laser track. First, each glass sample was irradiated using two different laser writing configurations: laser writing polarization parallel (along y) and perpendicular (along x) to the scanning direction (along y). Consequently, polarized optical microscopy (Olympus BX51) was used to quantify the birefringence response, along with its sensitivity (neutral axis orientation, amplitude) with respect to light polarization orientation, characteristic of nanogratings. Additionally, a complementary electron microscopy analysis (FEG–SEM Zeiss Supra 55 VP) was performed on the laser tracks (x,z plane) to ensure the existence of porous nanolayers and nanopores, therefore confirming the polarized optical microscopy results.

The data taken for all commercial glasses investigated were provided by the glass suppliers (technical datasheets). Additionally, the glass viscosities temperature dependence ($\eta(T)$) was fitted using the Vogel–Fulcher–Tammann (VFT) equation. The viscosity data for GeO_2 were taken from [31], [32] while other parameters were taken from [33], [34]. Most of the collected viscosity data points, in log(η, in Pa·s), are comprised between 3 and 13. Outside this interval the value of viscosity is less known.

III. Results and discussion

III.1. Domain of nanogratings existence

The formation of nanogratings in the E_p – RR landscape was investigated for SiO_2 (Suprasil), GeO_2, Borofloat 33, AF32, and BK7 glasses. The domain of nanogratings existence for each glass is shown in Fig. 1(a). As can be observed, the glass material strongly influences the ability to imprint nanogratings from the "self-organized" plasma. For BK7, which presents the smallest nanogratings window, porous nanogratings could be observed nevertheless, as shown in Fig. 1(b), but for very specific conditions (<100 kHz, and for typ. 50,000 pulses/µm). Additionally, and for all glasses, an example of measured retardance values (i.e., birefringence x nanogratings length along z axis) with respect to energy and at a constant RR = 50 kHz is provided in Fig. 1(c). Each measured retardance data point has a ± 5 nm uncertainty. The nanogratings window is the largest for SiO_2, intermediate for GeO_2, Borofloat 33, and AF32, and is extremely reduced for BK7 (an alkali "rich" borosilicate). Correspondingly, much higher values of retardance are found in silica glass compared to AF32 and BK7, which agree with the tendency to form nanogratings more easily in SiO_2 or GeO_2 that are strong network formers.

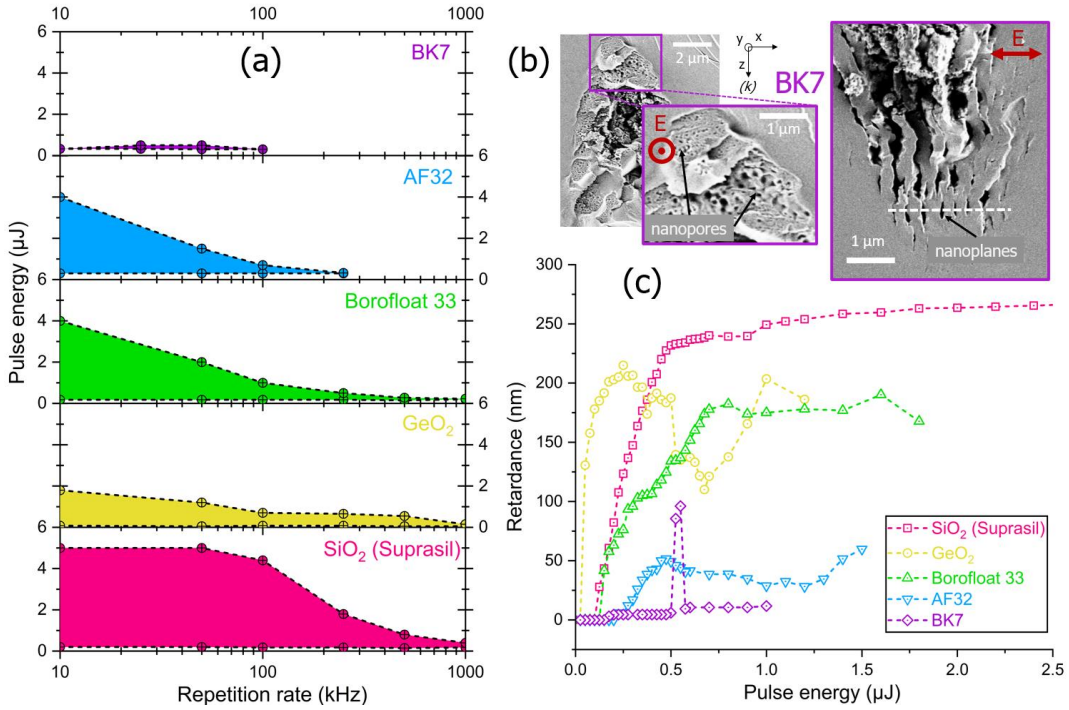

Fig. 1. a) Determination of observed nanogratings in an energy-repetition rate landscape for five glasses: SiO_2 (Suprasil), GeO_2, Borofloat 33, AF32, and BK7. b) Illustration of nanogratings observed in BK7 from scanning electron microscopy analysis; conditions are pulse duration = 800 fs, writing speed = 1 µm/s, RR = 25 kHz, E_p = 0.6 µJ, focal depth = 300 µm. c) Evolution of retardance as a function of pulse energy (800 fs, 50 kHz, NA = 0.6); each data point has a ± 5 nm uncertainty.

The principal aim of this paper is to highlight the link between nanogratings window and glass viscosity behavior with temperature. Therefore, and to better appreciate the discussion in the next Section, below is briefly discussed how the temperature elevation upon fs-laser irradiation is impacted in an E_p – RR landscape. There exist two principal situations when considering the E_p – RR landscape as in Fig. 1(a):

i) Low RR, increasing E_p. From the heat equation (Fourier's law), the temperature profile distribution in space is unchanged, but the deposited heat inside the material would increase. Consequently, the maximal temperature increase (ΔT) at the pulse center would also increase, following a general form of $\Delta T \sim aE_p/\rho C_p V$. Here a is the fraction of the pulse energy absorbed by the material and effectively transmitted to the glass phonons, ρ and C_p, respectively, are the glass density and heat capacity, and V the volume within which the pulse energy is

absorbed. It is worth pointing out that α is a function of fluence (e.g., in silica glass [35]), and such temperature rise has already been investigated for several glass matrices including silica or Borofloat 33 [36], [37]. As E_p is increased (and so ΔT), the spatial volume for which the temperature is beyond a transformation temperature threshold (e.g., formation of nanogratings) would be enlarged.

ii) High RR, fixed E_p. This condition is also called "heat accumulation regime". In this regime, the heat generated by a pulse in the irradiated area does not have enough time to fully diffuse away before the next pulse is delivered. This effect would typically result into an increase of the average temperature, hence a decrease of the glass viscosity, in the heat affected zone. The characteristic time to evacuate the heat can be estimated as $\tau_{th} \approx \omega_0^2/(D_{th})$, where $D_{th} = \kappa/(\rho C_p)$ is the diffusion coefficient, κ is the thermal conductivity, and ω_0 is the characteristic length corresponding to the beam waist radius at an intensity of $1/e^4$ (typ. 1.5 µm). As an example, this gives D_{th} (SiO_2) ≈ 8.9×10^{-7} m²/s and D_{th} (BK7) ≈ 5.2×10^{-7} m²/s, and consequently τ_{th} (SiO_2) ≈ 2.5 µs while τ_{th} (BK7) ≈ 4.3 µs. Turning these values into heat accumulation threshold frequencies, this gives f_{th} (SiO_2) ≈ 400 kHz and f_{th} (BK7) ≈ 230 kHz. Consequently, one would expect heat accumulation to be more pronounced in BK7 with respect to SiO_2.

From this short discussion and circling back to Fig. 1(a), one can note that the narrowing of the nanogratings window typically comes from both lower E_p and RR values. Consequently, the "temperature sensitivity" or "temperature interval" to make nanogratings appears reduced in glasses such as BK7 with respect to SiO_2. This reasoning is the starting point of the next Section dedicated to establishing a rational approach.

III.2. Rationale for a viscosity-based approach

Both the mechanisms of cavitation and erasure of the nanogratings take their roots in the material ability to break and reform itself in a time-temperature frame. In the following Section, the upper and lower limits of nanogratings existence are discussed on a temperature dependent viscosity basis.

Minimum viscosity to induce cavitation

When ultrashort laser pulses are deposited inside a large bandgap oxide glass as in our case, the pulse energy is absorbed by the glass material mostly through nonlinear effects (multi-photon absorption and tunnel ionization) and a significant part is subsequently transformed into heat through electron-lattice energy transfer. This takes a maximum of few 10s of picoseconds in most glasses [4], [38], while the maximum temperature increases as already discussed in the previous Section, reaching typically values of few thousands of degrees [36], [37]. For small-to-moderate pulse energy values, the generated heat cannot escape the irradiated volume in the time of a pulse duration (typ. 100-1000 fs). This is the condition of so-called "thermal confinement". For such condition to be valid, the pulse duration τ_p must be shorter than the thermal relaxation time τ_{th} [39]. As calculated above, for silica $\tau_{th} \approx 2.5$ µs and therefore $\tau_p << \tau_{th}$ for fs or ps laser pulses. The criterion of thermal confinement is thus satisfied. Additionally, if there are no significant strain or volume changes of the medium during heating, we are in the condition of so-called "stress confinement" [39]. For this second condition to be valid, the required time for the pulse to heat the sample must be shorter than the characteristic acoustic relaxation time $\tau_{ac} \approx 2\omega_0/c_s$, with c_s being the sound speed (≈ 6000 m/s for silica glass). This gives $\tau_{ac} \approx$ 500 ps whereas the electron-phonon coupling time is on the order of 10 ps for silica and therefore the criterion of stress confinement is also satisfied. Therefore, the experimental conditions are met to yield nanocavitation in the glass samples.

Subsequently to this and following the wave equation from isotropic solids, the maximum tensile stress internally developed can be approximated as $p \approx B\beta\Delta T$. Here B is the bulk modulus (36 GPa for silica), β is the volumetric expansion coefficient ($\beta \approx 3\alpha \approx 3\times5.5\times10^{-7}$ K^{-1} for silica), and ΔT is the temperature elevation following the pulse energy deposition. Some caveats are worth pointing out: we use solid properties for each material (bulk modulus, thermal expansion coefficient), and assume them constant with respect to temperature. Although this is questionable, it provides a guideline for reasoning. Interestingly, it must be pointed out that the resulting tensile stress is drastically different depending on the glass material considered. We must point out that at low pulse densities, nanopores are initially formed but no nanogratings, close to the so-called Type X regime [40], [41]. Before the onset of this regime, formed nanopores are dispersed, disordered, and quasi-spherical. The asymmetry of the nanopores is progressively reinforced during the self-organization and the formation of the nanogratings, mostly due to the action of light (and its polarization orientation and state), but not a stress field asymmetry. Additionally, the geometry of the heat affected zone can impact the overall energy deposition volume, and consequently temperature rise and stress distribution. However, here we consider nanopores of the size of few 10s of nm, which is much smaller than the irradiated volume (10s of μm^3). Therefore, it is quite reasonable to

consider as a first approximation that at some places inside the irradiated volume, the volume expansion and induced pressure are isotropic, similar to a hydrostatic pressure as a first approximation.

For a moderate temperature increase (e.g., 1000 °C [37]), there is an order of magnitude difference between p values for silica (≈ 60 MPa) and BK7 (≈ 1160 MPa). Once the tensile stress is developed, a positive pressure difference exists between the initiated pore and the surrounding material. Beyond a certain critical tension, the heated glass volume is expected to experience cavitation [16], [17]. For silica glass, Rudenko *et al.* demonstrated that the minimal temperature for cavitation is set when the viscosity is on the order of 10^6 Pa·s [17], [18]. Such temperature is very close to the softening point (T_{soft}) of the material, i.e., $10^{7.6}$ P or $10^{6.6}$ Pa·s, 1873 K for Suprasil. This temperature of cavitation is calculated for a viscosity of $\eta_{cav} \approx B\xi\tau_{th}^2 \approx 10^{6.3}$ Pa·s for silica, using a strain rate of $\xi = 10^7 s^{-1}$, so indeed close to the softening temperature as previously stated. In this work we use $\xi \approx p/(B \times \tau_{ac})$ which falls within the magnitude of η_{cav} values provided by Rudenko *et al.* [17], [18]. Written only in terms of glass and laser parameters, this gives $\eta_{cav} \approx p \times \left(\frac{\tau_{th}^2}{\tau_{ac}}\right) = \frac{\omega_0^3 \cdot p \cdot c_s}{2 \cdot D_{th}^2} = \frac{\omega_0^3 \cdot 3\alpha \cdot B \cdot \Delta T \cdot c_s \cdot \rho^2 \cdot c_p^2}{2\kappa^2}$. Some key properties, from the above discussion, are provided in Table 1. It is worth mentioning that for a constant p value (e.g., 100 MPa), η_{cav} is comprised between $10^{6.1}$ and $10^{6.6}$ Pa·s for all glasses considered. The cavitation temperature (T_{cav}) in Table 1 deduced from the VFT fit performed for each glass is found close to T_{soft}.

Table 1 Typical values including cavitation and erasure criteria and temperatures for the glasses investigated.

Glass material	$p \approx B \cdot \beta \cdot \Delta T^{1,2}$ (MPa)	$\log(\eta_{cav}, Pa{\cdot}s) \approx \log\left(p \cdot \left(\frac{\tau_{th}^2}{\tau_{ac}}\right)\right)$	T_{cav} (T_{soft}) (°C)	$\log(\eta_{max}, Pa{\cdot}s) \approx \log(p \cdot \tau_{th})$	T_{max} (°C)	T_{max} - T_{cav} (°C)
SiO_2 (Suprasil)	60	5.9	1688 (1600)	2.2	2298	610
GeO_2	440	7.1	838 (894)	3.3	1332	494
Borofloat 33	350	6.9	797 (821)	3.1	1254	457
AF32	550	7.1	937 (969)	3.2	1277	340
BK7	1160	7.6	675 (720)	3.7	906	231

[1]: Given for a ΔT value of 1000 °C, and p is a tensile (negative) pressure.

[2]: Data for B and β (with $\beta = 3\alpha$) can be found in the technical datasheet provided by the glass manufacturers, and in [33] and [34] for GeO_2.

Maximum viscosity before growth instability or erasure of nanogratings

Following the formation of nanopores beyond the cavitation temperature, the stability of a cavitated pore, i.e., its ability to exist, must be considered. From this view, one must investigate what are the key mechanisms that drive the pore size evolution (either its growth or collapse) once it is formed. This can be achieved through the analysis of the non-dimensional Rayleigh-Plesset (R-P) equation, which takes the following form [42]:

$$(\bar{R})\ddot{\bar{R}} + \frac{3}{2}\left(\dot{\bar{R}}\right)^2 = -\left(\frac{\tau}{\tau_p}\right)^2 \frac{p_\infty(t) - p_v}{p_{\infty\, ref} - p_v} - \left(\frac{\tau}{\tau_s}\right)^2 \frac{1}{\bar{R}} - \frac{\tau}{\tau_v}\frac{\dot{\bar{R}}}{\bar{R}} \qquad (1),$$

where $\bar{R} = R/a$ is a dimensionless radius near unity (a is a characteristic length, typ. the initial pore radius in few or tens of nm), τ is the characteristic time of bubble evolution (typically ns to µs as per the thermal diffusion timescale), $p_{\infty\, ref}$ is the reference pressure taken far away from the pore, p_v the pressure inside the pore ($p_{\infty\, ref} - p_v = p$ as defined above), and $\dot{\bar{R}}$ and $\ddot{\bar{R}}$ are the first and second derivatives of the radius with respect to time. In the above equation three characteristic times are set originating from: pressure $\left(\tau_p = a\sqrt{\frac{\rho}{p}}\right)$, viscosity $\left(\tau_v = \frac{\rho a^2}{4\eta}\right)$, and surface tension $\left(\tau_s = a\sqrt{\frac{\rho a}{2\sigma}}\right)$ with σ being the surface tension, taken constant with respect to temperature [42]. These characteristic times can be plotted as a function of the pore radius, as shown in Fig. 2. At this stage, few aspects on the R-P equation must be specified. First, the R-P equation is employed here as a simple tool to investigate the relationship between viscosity and nanogratings existence. In this work, the effect of temperature is taken into account through the viscosity term. However, during laser irradiation, temperature gradients are present, mostly due to the laser intensity distributed profile, and consequently its associated energy deposition and heat transfer. This can be a function of both laser parameters (e.g., pulse energy and duration, repetition rate etc.) but also material properties, including bandgap energy, photoionization rate, nonlinear absorption coefficient, etc. Consequently, a reliable estimate of temperature distribution within irradiated area remains quite difficult. Nevertheless, the R-P equation still provides interesting aspects of reasoning with respect to temperature effects and enables qualitative understanding of the main driven forces involved in the glasses during nanogratings formation. For instance, this equation was successfully applied to predict the erasure of nanopores during

isochronal thermal annealing for a series of silicate glasses [43]. For completeness, we pinpoint that cavitation could also originate from a nucleation and liquid-vapor phase transformation. While the focus of this work essentially emphasizes the link between viscosity and the existence of nanopores, other cavitation mechanisms than a spall-induced cavitation can be envisioned.

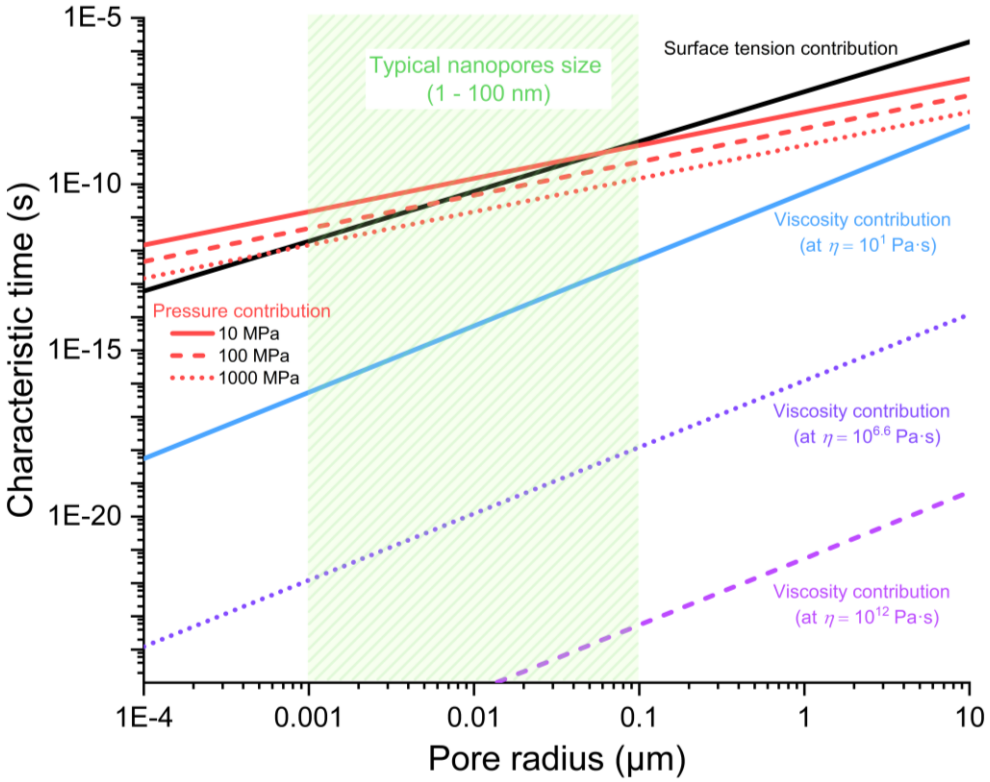

Fig. 2. Evolution for characteristic time as a function of pore radius using the non-dimensional Rayleigh-Plesset equation. The impact of pressure (set at Δp = 10, 100, 1000 MPa), surface tension (with σ = 0.3 J/m^2), and viscosity can be estimated (the contribution with the smallest characteristic time dominates).

Turning back to the characteristic times provided above and calculated in Fig. 2, the contribution holding the lowest characteristic time (i.e., the slowest process) is the limiting (i.e., driving) factor in the evolution of the nanopores. Typical values for silica at the softening point ($10^{6.6}$ Pa·s) for a 5 nm pore radius would give $\tau_v \approx 10^{-21}$ s, τ_s and $\tau_p \approx 10^{-11}$ s. At the melting temperature (defined as 10^{1} Pa·s) $\tau_v \approx 10^{-15}$ s, which is still 4 orders of magnitude lower than τ_p. It is indicative that the dynamics of nanopore evolution (growth/collapse) is almost exclusively driven by glass viscosity. For completeness, τ_v is proportional to $1/\eta$. Consequently, if the experimental characteristic time is lower than τ_v, the process would not depend on viscosity. In our situation, a realistic nanopores erasure timescale would be in the ns to μs (as per typical thermal diffusion times). Therefore, the viscosity is expected to primarily drive the nanopores size evolution. This is even more valid as the viscosity is increased, yielding to lower values of τ_v.

Consequently, a criterion must be selected as an indication of pore instability. The use of the dimensionless Peclet number (Pe) was proposed to set the limit of "unstable" hydrodynamic growth of the nanopores [44]. The limit is set for $Pe = \frac{p \times \tau_{th}}{\eta_{max}} = 1$, giving the criterion $\eta_{max} \sim p \times \tau_{th}$. For silica glass it gives a value of ~$10^{2.2}$ Pa·s, corresponding to a $T \sim 2300$ °C. The calculated η_{max} for the glasses considered in this study are reported in Table 1. The η_{max} value corresponds to the maximal viscosity beyond which a viscous growth would prevent stable nanopores to exist. All the glasses fall within a η_{max} interval of $10^{2.2}$ - $10^{3.7}$ Pa·s. Finally, it is worth pointing out that the stress induced upon heating will ultimately relax, yielding to a drop in the initial tensile pressure p. From this perspective and the above equation, one can notice that η_{max} would be lower. Therefore, a potential collapse of the pore is anticipated if the pressure contribution becomes less important than that of the surface tension term [42], [45]. This competing effect is exemplified in Fig. 2, where low pressures such as 10 MPa would tend to promote collapse ($\tau_p > \tau_s$), while higher pressures such as 1000 MPa would yield to growth ($\tau_p < \tau_s$). In an intermediate regime, the pore could experience either growth or collapse, and perhaps both within the laser track location. This suggests that there may be a competing effect between pore growth and

collapse depending on the temperature/viscosity and conditions considered. However, beyond η_{max} the existence of nanopores is expected to be compromised and this viscosity value is kept as the upper bound of nanogratings existence.

III.3. Prediction of nanogratings imprinting in various glass systems

From the above discussion, it becomes clear that the temperature difference between the T_{max} and T_{cav}, reported in Table 1, must be maximized for a glass in order to present a larger nanogratings window. In Fig. 3(a) the viscosity as a function of temperature for multiple oxide glasses (in addition to the ones discussed in this paper) is reported. An estimated domain of nanogratings existence is provided in Fig. 3(b), by taking the temperature difference between T_{max} (set as $\eta = 10^{3.0}$ Pa·s) and T_{soft} ($\eta = 10^{6.6}$ Pa·s), respectively upper and lower bounds.

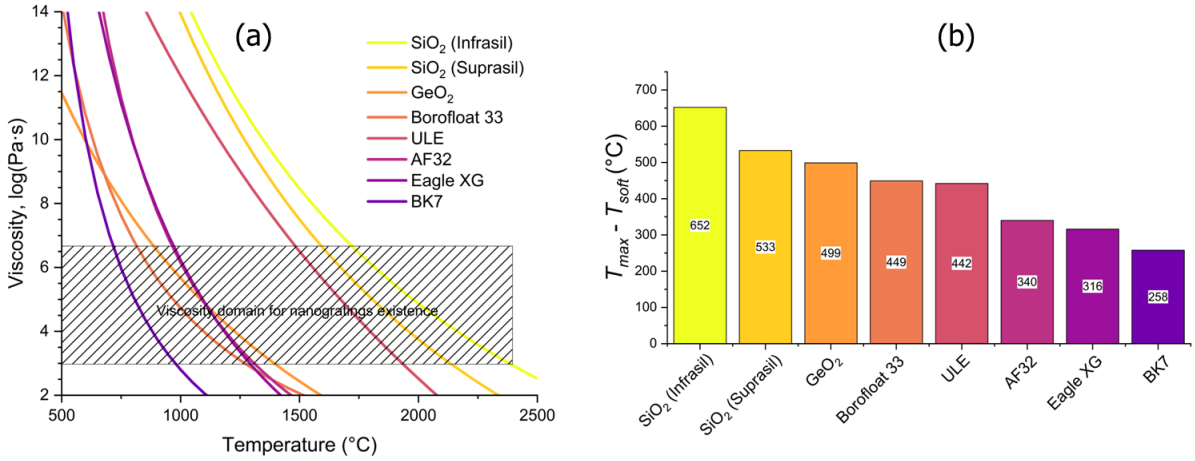

Fig. 3. a) Viscosity as a function of temperature for a variety of commercial and typical glasses, along with an estimated domain of nanogratings existence from T_{soft} ($\eta = 10^{6.6}$ Pa·s) to T_{max} ($\eta = 10^{3.0}$ Pa·s). b) Temperature difference ($T_{max} - T_{soft}$) as a function of glass composition. A larger value suggests a wider processing window (with respect to temperature) to form nanogratings.

The predicted "effectiveness" to imprint "stable" nanogratings in the selected glasses, in a sense that they can be observed after laser irradiation, agrees with the results reported in Fig. 1, where BK7 presents the lowest temperature interval and the narrowest nanogratings window, while it is the opposite for silica. Moreover, these findings concur with literature data. For example, in Ref. [26], for 800 fs pulse duration, the nanogratings window was found larger for SiO_2, the Borofloat 33, and finally AF32, which is what is found and predicted herein (Figs. 1a and 3b). In GeO_2 and GeO_2-doped SiO_2 glasses, it was found relatively easy to induce nanogratings with various sets of laser parameters and writing conditions [20]–[22], [24], [25]. Moreover, the birefringence response observed in Ref. [27] for BK7 was likely due to nanogratings. Indeed, from this work we demonstrated the nanogratings imprinting in BK7 through SEM observations (Fig. 1b), while both the experimentally and predicted narrow nanogratings windows agree with the difficulty in this cited work to detect the nanopores/nanoplanes using scanning electron microscopy.

Several other aspects are worth discussing. First, BK7 displays a much lower bandgap energy compared to silica (~3.5 eV versus ~9 eV). Consequently, even with a 3-photon nonlinear absorption (in our case $\lambda = 1030$ nm, i.e., 1.2 eV), the formation of bulk nanogratings is still possible. Secondly, in some glasses such as alkali-rich glasses (e.g., Na_2O-SiO_2 [23]) a large number of pulses (multi-pulse regime) is required to trigger nanogratings (typ. > 10^5 or 10^6 pulses). Interestingly, network modifiers are found to migrate outward of the irradiated volume [30]. A direct consequence, based on our work, could be a local variation in the glass viscosity enabling not only the formation of nanogratings at short timescale but also their survival to the heating-cooling processes during pulse deposition. Moreover, contrarily to LIPSS, the formation of nanogratings still requires a multi-pulse regime even for silica [23], [28]. As mentioned earlier in this paper, at low pulse energies or pulse densities, a regime (so-called Type X) was identified where nanopores can exist, but the nanogratings are not formed yet. At this stage of the process, the nanopores are not highly elongated yet and self-organized into nanolayers [41], [46]. Interestingly, this regime suggests that the cavitation process can already take place after the first few pulses are being deposited. In fact, this work anticipates cavitation after the very first pulses are deposited, and therefore takes the Type X into account. Furthermore, the heat accumulation process, as discussed in section III.1 and triggered by a multi-pulse regime, may play a direct role in the formation and erasure of these pores through an increase of temperature in

the heat affected region. We therefore expect that the minimum pulse density to induce nanogratings would be a strong function of glass composition.

For completeness, several studies have highlighted, based on thermo-mechanical arguments, strong evidences of a void-to-nanogratings transitioning upon progressive laser irradiation (e.g., Refs. [47], [48]). Although this requires a more in-depth analysis based on the proposed approach, several aspects are anticipated herein. High tensile strength, generated by high energy deposition, would favor voids formation as the pressure contribution would overcome the surface energy term (Fig. 3), yielding viscous growth of the nanopores. Additionally, the description of higher thermal gradients, associated with the fastest growth of nanobubbles in the laser track head as described in Ref. [48], is in agreement with our findings. While the topic of another study, this approach could also frame the existence domain of voids-like transformations.

Finally, no direct observation of porous bulk nanogratings has been reported for other glass systems. However, recently sub-surface formation of nanopores revealed to be possible under specific conditions in tellurite or chalcogenide glasses [49], [50]. This might be because the viscosity of these glasses strongly varies with respect to temperature (short glasses). This would further narrow the nanogratings window and compromise nanogratings formation, in agreement with the presently advocated viscosity approach. For crystalline structures, such as in Al_2O_3 [51] or TeO_2 [52], the laser-induced modifications would depend on the internal structure of the nanogratings (nanopores, nanoscale phase separation, or local amorphization or recrystallization etc….). Additionally, for crystals the viscosity would be abruptly reduced above the melting temperature as the material transits from crystal to liquid phase. This is much different from glasses, which exhibit a progressive decrease in viscosity as the temperature increases. Hence, at this step our approach is restricted to nanogratings made of nanopores. Still, we expect that the latter can be broaden to other types of nanogratings, since chemical migration and crystallization kinetics include mobility, and consequently viscosity-related phenomena.

IV. Conclusion

Understanding the formation of nanogratings inside silicate and germanate glasses is an attractive research field, since these sub-wavelength and self-organized structures enable miniaturized functionalization and unique properties. In this context, this work addresses the challenges to imprint, or not, nanogratings, through a viscosity approach. It is shown, building from previous work, that the nanogratings domain is bound between two limits: i) a low temperature one, corresponding to a cavitation mechanism, and for which the viscosity is situated at $\sim 10^{6.6}$ Pa·s, and ii) a high temperature one when the pores experience either growth or collapse, this time for a viscosity value typically around $\sim 10^{3.0}$ Pa·s. These predictions are validated by experimental work performed on five glasses, for which nanogratings domains are either large (SiO_2), intermediate (GeO_2, AF32, Borofloat 33), and narrow (BK7). The results agree with the literature and the proposed viscosity approach. A direct consequence of this work is to demonstrate that nanogratings can be achieved in most, if not any, glasses. However, the processing windows can be drastically different, and a systematic analysis must be undertaken to find the adequate conditions for which nanogratings can survive the laser-irradiation process.

Future work includes simulation of the temperature elevation during the irradiation process for each glass composition. This will help to target and anticipate in which conditions the temperature range, hence viscosity range (see Fig. 3) corresponding to the formation of nanogratings, can be achieved.

Funding

This research was funded by Agence Nationale pour la Recherche, FLAG-IR project, grant number ANR-18-CE08-0004-01 and CNRS Défi Instrumentation aux Limites, UltraBragg project. Qiong Xie acknowledges the China Scholarship Council (CSC) for the funding of her PhD fellowship.

References

[1] Y. Shimotsuma, P. G. Kazansky, J. Qiu, and K. Hirao, "Self-Organized Nanogratings in Glass Irradiated by Ultrashort Light Pulses," *Phys. Rev. Lett.*, vol. 91, no. 24, pp. 247405(1)-247405(4), Dec. 2003, doi: 10.1103/PhysRevLett.91.247405.

[2] J. Tian *et al.*, "Spectral dependence of femtosecond laser induced circular optical properties in silica," *OSA Contin.*, vol. 2, no. 4, pp. 1233–1242, 2019, doi: 10.1364/osac.2.001233.

[3] J. Tian, M. Lancry, B. Poumellec, E. Garcia-Caurel, and R. Ossikovski, "Study of femtosecond laser induced circular optical properties by Mueller matrix spectropolarimetry," *Opt. Lett.*, vol. 42, no. 20, pp.

4103–4106, 2017, doi: 10.1364/ol.42.004103.
[4] E. Mazur and R. Gattass, “Femtosecond laser micromachining in transparent materials,” *Nat. Photonics*, vol. 2, no. 4, pp. 219–225, 2008, doi: 10.1038/nphoton.2008.48.
[5] S. J. Mihailov *et al.*, “Extreme Environment Sensing Using Femtosecond Laser-Inscribed Fiber Bragg Gratings,” *Sensors*, vol. 17, no. 12, 2017, doi: 10.3390/s17122909.
[6] B. Zhang, X. Liu, and J. Qiu, “Single femtosecond laser beam induced nanogratings in transparent media - Mechanisms and applications,” *J. Mater.*, vol. 5, pp. 1–14, 2019, doi: .1037//0033-2909.I26.1.78.
[7] Y. Shimotsuma *et al.*, “Ultrafast manipulation of self-assembled form birefringence in glass,” *Adv. Mater.*, vol. 22, no. 36, pp. 4039–4043, 2010, doi: 10.1002/adma.201000921.
[8] M. Beresna, M. Gecevičius, and P. G. Kazansky, “Polarization sensitive elements fabricated by femtosecond laser nanostructuring of glass [Invited],” *Opt. Mater. Express*, vol. 1, no. 4, pp. 783–795, 2011, doi: 10.1364/ome.1.000783.
[9] R. Stoian, “Volume photoinscription of glasses: three-dimensional micro- and nanostructuring with ultrashort laser pulses,” *Appl. Phys. A Mater. Sci. Process.*, vol. 126, no. 6, pp. 1–30, 2020, doi: 10.1007/s00339-020-03516-3.
[10] R. Taylor, C. Hnatovsky, and E. Simova, “Applications of femtosecond laser induced self-organized planar nanocracks inside fused silica glass,” *Laser Photonics Rev.*, vol. 2, no. 1–2, pp. 26–46, 2008, doi: 10.1002/lpor.200710031.
[11] M. Beresna, M. Gecevičius, P. G. Kazansky, T. Taylor, and A. V. Kavokin, “Exciton mediated self-organization in glass driven by ultrashort light pulses,” *Appl. Phys. Lett.*, vol. 101, no. 5, pp. 053120(1)-053120(4), 2012, doi: 10.1063/1.4742899.
[12] R. Buschlinger, S. Nolte, and U. Peschel, “Self-organized pattern formation in laser-induced multiphoton ionization,” *Phys. Rev. B - Condens. Matter Mater. Phys.*, vol. 89, no. 18, pp. 1–10, 2014, doi: 10.1103/PhysRevB.89.184306.
[13] A. Rudenko, J. P. Colombier, and T. E. Itina, “From random inhomogeneities to periodic nanostructures induced in bulk silica by ultrashort laser,” *Phys. Rev. B*, vol. 93, no. 7, pp. 075427(1)-075427(13), 2016, doi: 10.1103/PhysRevB.93.075427.
[14] J. Canning, M. Lancry, K. Cook, A. Weickman, F. Brisset, and B. Poumellec, “Anatomy of a femtosecond laser processed silica waveguide,” *Opt. Mater. Express*, vol. 1, no. 5, pp. 998–1008, 2011, doi: 10.1364/ome.1.000998.
[15] M. Lancry, B. Poumellec, J. Canning, K. Cook, J.-C. Poulin, and F. Brisset, “Ultrafast nanoporous silica formation driven by femtosecond laser irradiation,” *Laser Photonics Rev.*, vol. 7, no. 6, pp. 953–962, 2013, doi: 10.1002/lpor.201300043.
[16] D. E. Grady, “The spall strength of condensed matter,” *J. Mech. Phys. Solids*, vol. 36, no. 3, pp. 353–384, 1988.
[17] A. Rudenko, J. P. Colombier, and T. E. Itina, “Nanopore-mediated ultrashort laser-induced formation and erasure of volume nanogratings in glass,” *Phys. Chem. Chem. Phys.*, vol. 20, no. 8, pp. 5887–5899, 2018, doi: 10.1039/c7cp07603g.
[18] A. Rudenko, “Numerical study of ultrashort laser-induced periodic nanostructure formation in dielectric materials To cite this version : HAL Id : tel-02107355 Sciences Ingénierie et Santé Anton Rudenko Numerical study of ultrashort laser induced periodic,” 2019.
[19] M. Huang, F. Zhao, Y. Cheng, N. Xu, and Z. Xu, “Origin of laser-induced near-subwavelength ripples: Interference between surface plasmons and incident laser,” *ACS Nano*, vol. 3, no. 12, pp. 4062–4070, 2009, doi: 10.1021/nn900654v.
[20] M. Lancry *et al.*, “Nanogratings formation in multicomponent silicate glasses,” *Appl. Phys. B Lasers Opt.*, vol. 122, no. 3, pp. 1–8, 2016, doi: 10.1007/s00340-016-6337-8.
[21] F. Zimmermann *et al.*, “Femtosecond laser written nanostructures in Ge-doped glasses,” *Opt. Lett.*, vol. 41, no. 6, pp. 1161–1164, 2016, doi: 10.1364/ol.41.001161.
[22] M. Lancry, J. Canning, K. Cook, M. Heili, D. R. Neuville, and B. Poumellec, “Nanoscale femtosecond laser milling and control of nanoporosity in the normal and anomalous regimes of GeO2-SiO2 glasses,” *Opt. Mater. Express*, vol. 6, no. 2, pp. 321–330, 2016, doi: 10.1364/OME.6.000321.
[23] S. Lotarev, S. Fedotov, A. Lipatiev, M. Presnyakov, P. Kazansky, and V. Sigaev, “Light-driven nanoperiodical modulation of alkaline cation distribution inside sodium silicate glass,” *J. Non. Cryst. Solids*, vol. 479, no. October, pp. 49–54, 2018, doi: 10.1016/j.jnoncrysol.2017.10.008.
[24] F. Zhang, H. Zhang, G. Dong, and J. Qiu, “Embedded nanogratings in germanium dioxide glass induced by femtosecond laser direct writing,” *J. Opt. Soc. Am. B*, vol. 31, no. 4, p. 860, 2014, doi: 10.1364/josab.31.000860.
[25] J. Wang, X. Liu, Y. Dai, Z. Wang, and J. Qiu, “Effect of sodium oxide content on the formation of nanogratings in germanate glass by a femtosecond laser,” *Opt. Express*, vol. 26, no. 10, p. 12761, 2018, doi: 10.1364/oe.26.012761.

[26] S. S. Fedotov *et al.*, "Direct writing of birefringent elements by ultrafast laser nanostructuring in multicomponent glass," *Appl. Phys. Lett.*, vol. 108, no. 7, 2016, doi: 10.1063/1.4941427.
[27] S. Richter *et al.*, "Laser induced nanogratings beyond fused silica - periodic nanostructures in borosilicate glasses and ULE™," *Opt. Mater. Express*, vol. 3, no. 8, pp. 1161–1166, 2013, doi: 10.1364/OME.3.001161.
[28] S. Richter, M. Heinrich, S. Döring, A. Tünnermann, S. Nolte, and U. Peschel, "Nanogratings in fused silica: Formation, control, and applications," *J. Laser Appl.*, vol. 24, no. 4, pp. 042008(1)-042008(8), 2012, doi: 10.2351/1.4718561.
[29] Y. Wang, M. Cavillon, N. Ollier, B. Poumellec, and M. Lancry, "An Overview of the Thermal Erasure Mechanisms of Femtosecond Laser-Induced Nanogratings in Silica Glass," *Phys. Status Solidi Appl. Mater. Sci.*, vol. 218, no. 12, pp. 2100023(1)-2100023(15), 2021, doi: 10.1002/pssa.202100023.
[30] T. T. Fernandez *et al.*, "Bespoke photonic devices using ultrafast laser driven ion migration in glasses," *Prog. Mater. Sci.*, vol. 94, pp. 68–113, 2018, doi: 10.1016/j.pmatsci.2017.12.002.
[31] S. K. Sharma, D. Virgo, and I. Kushiro, "Relationship between density, viscosity and structure of GeO2 melts at low and high pressures," *J. Non. Cryst. Solids*, vol. 33, no. 2, pp. 235–248, 1979, doi: 10.1016/0022-3093(79)90052-8.
[32] E. M. Birtch, J. E. Shelby, and J. M. Whalen, "Properties of binary GeO_2 – SiO_2 glasses," *Phys. Chem. Glas.*, vol. 47, no. 2, pp. 182–185, 2006.
[33] M. J. Weber, *Handbook of Optical Materials*, vol. 23, no. 1. CRC Press, 2003.
[34] E. M. Dianov and V. M. Mashinsky, "Germania-based core optical fibers," *J. Light. Technol.*, vol. 23, no. 11, pp. 3500–3508, 2005, doi: 10.1109/JLT.2005.855867.
[35] B. Momgaudis, V. Kudriasov, M. Vengris, and A. Melninkaitis, "Quantitative assessment of nonlinearly absorbed energy in fused silica via time-resolved digital holography," *Opt. Express*, vol. 27, no. 5, pp. 7699–7711, 2019, doi: 10.1364/oe.27.007699.
[36] M. Shimizu *et al.*, "Three-dimensional temperature distribution and modification mechanism in glass during ultrafast laser irradiation at high repetition rates," *Opt. Express*, vol. 20, no. 2, pp. 934–940, 2012, doi: 10.1364/oe.20.000934.
[37] T. Yoshino, Y. Ozeki, M. Matsumoto, and K. Itoh, "In situ micro-raman investigation of spatio-temporal evolution of heat in ultrafast laser microprocessing of glass," *Jpn. J. Appl. Phys.*, vol. 51, no. 10, 2012, doi: 10.1143/JJAP.51.102403.
[38] L. Orazi, L. Romoli, M. Schmidt, and L. Li, "Ultrafast laser manufacturing: from physics to industrial applications," *CIRP Ann. - Manuf. Technol.*, vol. 00, pp. 1–24, 2021, doi: 10.1016/j.cirp.2021.05.007.
[39] G. Paltauf and P. E. Dyer, "Photomechanical processes and effects in ablation," *Chem. Rev.*, vol. 103, no. 2, pp. 487–518, 2003, doi: 10.1021/cr010436c.
[40] P. Kazansky, M. Sakakura, and L. Wang, "Method for fabricating nanostructured optical elements using polarised light," US 2022/0009028 A1, 2022.
[41] M. Sakakura, Y. Lei, L. Wang, Y. H. Yu, and P. G. Kazansky, "Ultralow-loss geometric phase and polarization shaping by ultrafast laser writing in silica glass," *Light Sci. Appl.*, vol. 9, no. 1, pp. 1–10, 2020, doi: 10.1038/s41377-020-0250-y.
[42] J.-P. Franc, "The Rayleigh-Plesset equation: a simple and powerful tool to understand various aspects of cavitation," in *Fluid Dynamics of cavitation and cavitating turbopumps*, vol. 496, 2007, pp. 1–41.
[43] M. Cavillon, Y. Wang, B. Poumellec, F. Brisset, and M. Lancry, "Erasure of nanopores in silicate glasses induced by femtosecond laser irradiation in the Type II regime," *Appl. Phys. A*, vol. 126, no. 11, pp. 876(1)-876(9), Nov. 2020, doi: 10.1007/s00339-020-04062-8.
[44] A. Rudenko *et al.*, "Spontaneous periodic ordering on the surface and in the bulk of dielectrics irradiated by ultrafast laser: A shared electromagnetic origin," *Sci. Rep.*, vol. 7, no. 1, pp. 1–14, 2017, doi: 10.1038/s41598-017-12502-4.
[45] M. S. Plesset, "The Dynamics of Cavitation Bubbles," *J. Appl. Mech.*, vol. 16, pp. 277–282, 1949, doi: 10.1080/15435075.2018.1431546.
[46] Y. Bellouard *et al.*, "Stress-state manipulation in fused silica via femtosecond laser irradiation," *Optica*, vol. 3, no. 12, pp. 1285–1293, 2016, doi: 10.1364/optica.3.001285.
[47] Y. Dai, A. Patel, J. Song, M. Beresna, and P. G. Kazansky, "Void-nanograting transition by ultrashort laser pulse irradiation in silica glass," *Opt. Express*, vol. 24, no. 17, p. 19344, 2016, doi: 10.1364/oe.24.019344.
[48] E. O. Kissi and Y. Bellouard, "Self-organized nanostructures forming under high-repetition rate femtosecond laser bulk-heating of fused silica," *Opt. Express*, vol. 26, no. 11, p. 14024, 2018, doi: 10.1364/oe.26.014024.
[49] G. Torun, T. Kishi, and Y. Bellouard, "Direct-write laser-induced self-organization and metallization beyond the focal volume in tellurite glass," *Phys. Rev. Mater.*, vol. 5, no. 5, pp. 1–10, 2021, doi: 10.1103/PhysRevMaterials.5.055201.

[50] G. Torun, A. Yadav, K. A. Richardson, and Y. Bellouard, “Ultrafast Laser Direct-Writing of Self-Organized Microstructures in Ge-Sb-S Chalcogenide Glass,” *Front. Phys.*, vol. 10, pp. 1–11, 2022, doi: 10.3389/fphy.2022.883319.
[51] D. Wortmann, J. Gottmann, N. Brandt, and H. Horn-Solle, “Micro-and nanostructures inside sapphire by fs-laser irradiation and selective etching,” *Opt. Express*, vol. 16, no. 3, pp. 197–200, 2008, doi: 10.1364/oe.16.001517.
[52] Y. Shimotsuma, K. Hirao, J. Qiu, and P. G. Kazansky, “Nano-modification inside transparent materials by femtosecond laser single beam,” *Mod. Phys. Lett. B*, vol. 19, no. 5, pp. 225–238, 2005, doi: 10.1142/S0217984905008281.